EFFECTS OF INTERFERENCE AND OXIDATION ON THE UV/VISIBLE REJECTION PROPERTIES OF FILTERS FOR SOFT X-RAY DETECTORS

M. BARBERA[1], A. COLLURA[2,1], A. DARA[1], M. LEONE[3], F.R. POWELL[4], S. SERIO[1], S. VARISCO[1] and M.V. ZOMBECK[5]
1. Istituto ed Osservatorio Astronomico G.S. Vaiana, Palermo
2. Istituto per le Applicazioni Interdisciplinari della Fisica (CNR), Palermo
3. Istituto di Fisica, Università degli Studi, Palermo
4. Luxel Corporation, Friday Harbor, WA
5. Harvard-Smithsonian Center for Astrophysics, Cambridge, MA

Submitted to Experimental Astronomy

Abstract. We report on UV/Visible transmission measurements of aluminum coated Lexan filters designed as UV blocking filters for soft x-ray detectors. Transmission of the filters in the $2300 - 8000$ Å wavelength range is significantly higher than expected. It cannot be accounted for applying a simple slab model of the transmission and adopting material properties reported in the literature. We show that this is due to interference effects which are strongly dependent on the filter geometry, and to oxidation of exposed aluminum surfaces and/or chemical interaction with the plastic support. The results of this work have led to the redesign of the Advanced X-ray Astrophysics Facility High Resolution Camera UV blocking filters.

Key words: X-ray, calibration, filters, interference, oxidation

1. Introduction

Aluminum coated Lexan filters are often used in x-ray astronomy instruments. They have been employed in the European X-ray Observatory Satellite (EXOSAT) (Taylor et al., 1981), the Röntgensatellit (ROSAT) (Truemper, 1983), and the Extreme Ultraviolet Explorer (EUVE) (Bowyer et al., 1992; Malina, 1992) as UV blocking filters for microchannel plate (MCP) detectors, and were baselined for the UV/Ion shields of the High Resolution Camera (HRC) (Murray and Chappel, 1985) on board the Advanced X-ray Astrophysics Facility (AXAF) (Weisskopf, 1985; Weisskopf, 1996).

Lexan ($C_{16}H_{14}O_3$, bisphenol-A polycarbonate) is a plastic material whose soft x-ray properties are well known (Fabricant et al., 1979). Nevertheless, in some cases where aluminum coated Lexan filters have been employed as UV blocking filters for soft x-ray detectors, leaks in the UV band have been detected during the in orbit operation. This was particularly evident and puzzling in the ROSAT mission where the High Resolution Imager (HRI) detected unexpectedly high count-rates from hot stars (Zombeck et al., 1995).

In this paper we report on UV and visible transmission measurements conducted on aluminum coated Lexan filters initially developed for the AXAF-HRC

UV/Ion shields. We show the occurrence of interferences in transmission at visible and UV wavelengths, due to the multilayer design of coated plastic membranes, that significantly reduce the UV opacity at resonant wavelengths. In addition, the oxidation of the exposed surfaces of aluminum and/or the occurrence of chemical interactions between aluminum and the plastic support also affect the UV/Visible opacity.

In section 2 we describe the vacuum UV and FUV/Visible transmission measurements conducted in the framework of this work. In section 3 we summarize the analytical approach we have used to model the observed interferences in transmission, while in section 4 we discuss a possible interpretation of the observed filter performances. Results and conclusions are summarized in section 5. In another paper we will discuss the implications of these results for the interpretation of the observed UV leak in the ROSAT HRI detector.

2. Measurements

All measured samples, manufactured by the Luxel Corporation (Friday Harbor, WA) , are listed in table I giving sample number (column 1), manufacturer ID number (column 2), sample material (column 3), manufacturer nominal thickness (column 4).

Table I
List of Measured Film Samples including manufacturer identification number, filter materials, and nominal thicknesses given by the manufacturer.

Sample	ID. NUM.	Material	Nominal Thickness (Å)		
			Al	Lexan	Al
1	TF101-952	Al-Lexan[1]-Al	360±35	6065±100	345±35
2	TF101-542	Al-Lexan[1]	710±50	5805±100	
3	TF110-380	Lexan[1]		5740±100	

[1]General Electric RL5002.

Vacuum UV transmission measurements were conducted at the XACT facility of the Osservatorio Astronomico di Palermo G.S. Vaiana (Collura et al., 1994; Collura et al., 1996) on sample 1 which was initially baselined as the UV/Ion shields for the imaging detector of the HRC on AXAF (HRC-I) (Murray and Chappel, 1985). This sample consists of a Lexan membrane coated with aluminum on both sides (see table I).

The adopted instrumental set-up consists of:

– A 1.0 m diameter grazing incidence monochromator (McPherson model 248/310 G) with 113 grooves per mm grating;

– Two interchangeable UV sources: 1) a windowless hollow cathode source (McPherson model 629) to cover the wavelength range 200-2500 Å, and 2) a mercury lamp which provides a bright calibration line at 2537 Å;
– Two interchangeable photon counting detectors: 1) a KBr coated microchannel plate (MCP) for wavelengths shorter than $\sim$ 1200 Å, and 2) a Far-UV photomultiplier tube (FUV PMT) with a cesium telluride photo-cathode for use at longer wavelengths;
– Two neutral density meshes* of nearly 1% transmission, which can be inserted in the beam one at a time or together to reduce the flux intensity.

Source power (dependent on gas pressure and high voltage supplied) and monochromator slits are set in order to never exceed the maximum count rate that the detectors can manage ($\sim$ 30000 cts/s for the MCP and $\sim$ 50000 cts/s for the FUV PMT). With these choices of slits' aperture, the typical pass band of the monochromator is about 5 Å FWHM. Data acquisition time intervals are typically in the range 1-100 minutes.

Transmission of the UV/Ion shields at the wavelengths of higher orders may be much higher than transmission at the wavelength of interest. For this reason, contamination from higher orders can significantly affect the measurement. In order to reduce this effect we have adopted the measurement technique described by Vallerga et al. (1986). At a few wavelengths the transmission of the film sample is below the sensitivity threshold of our instrumentation ($\sim 10^{-6} - 10^{-8}$ depending on wavelengths). For these cases only a 3 σ upper limit on transmission has been quoted. Table II lists the measured transmission of sample 1 at the surveyed wavelengths together with the source, gas, and detector used. Column 6 in table II reports expected transmission based on a simple slab transmission model adopting known linear attenuation coefficients of Lexan and aluminum (Barstow, 1985).

The thicknesses of Lexan and aluminum adopted to estimate predicted UV transmission were derived from x-ray transmission measurements conducted at the PTB laboratory of BESSY synchrotron (Barbera et al., 1996). The mass areal densities reported in table III have been derived from a least χ^2 fitting to the x-ray transmission measurements in the energy band 200-1950 eV, adopting a model of x-ray transmission that includes Lexan and aluminum. Thicknesses were derived from the mass areal densities using density values of 1.20 $g\ cm^{-3}$ and 2.5 $g\ cm^{-3}$ for Lexan and aluminum, respectively. The last column in table III gives the χ^2 value of the best fit to measured x-ray transmission (375 data points, relative statistical uncertainty = 0.0075 at all energies).

Figure 1 is a plot of measured vacuum UV transmission and upper-limits together with predictions from a simple slab transmission model adopting known linear

* In order to measure the transmission of UV blocking filters, high fluxes are required that could saturate the detectors. Neutral density meshes can be placed in the beam line to reduce the incident flux when the UV blocking filters are out.

Table II
Vacuum UV transmission measured at XACT on sample 1 together with adopted instrumental configuration (detector, source, source gas). Column 6 gives the expected transmission based on a simple slab transmission model with X-ray derived thickness of Lexan and aluminum.

Detector	Source	Gas	λ (Å)	Meas. Transm.	Expect. Transm.
MCP	Hollow Cathode	He	256.3	$(8.5 \pm 0.5)\ 10^{-6}$	$1.5\ 10^{-5}$
MCP	Hollow Cathode	He	303.8	$(1.5 \pm 0.1)\ 10^{-7}$	$1.8\ 10^{-7}$
MCP	Hollow Cathode	He	584.3	$< 4.5\ 10^{-9}$	$3.1\ 10^{-18}$
MCP	Hollow Cathode	Ar	919.8	$< 6.7\ 10^{-9}$	$5.6\ 10^{-19}$
FUV PMT	Hollow Cathode	He	1640.5	$< 9.5\ 10^{-6}$	$3.3\ 10^{-9}$
FUV PMT	Hollow Cathode	CO	1657.2	$< 1.41\ 10^{-6}$	$3.3\ 10^{-9}$
FUV PMT	Hollow Cathode	CO	2190.4	$< 3.14\ 10^{-6}$	$3.2\ 10^{-10}$
FUV PMT	Hollow Cathode	CO	2300.6	$(1.6 \pm 0.3)\ 10^{-6}$	$1.2\ 10^{-8}$
FUV PMT	Hg lamp		2536.5	$(9.3 \pm 0.9)\ 10^{-4}$	$9.3\ 10^{-6}$

Table III
Best Fit results on synchrotron x-ray transmission measurements obtained adopting an x-ray transmission model which includes aluminum and Lexan

Sample	Mass Areal Density ($\mu g\ cm^{-2}$)		Derived Thickness (Å)		χ^2
	Al	Lexan	Al	Lexan	
1	18.2±0.2	75 ± 2	730±10	6290±100	3.17
2	15.2±0.2	71.9±0.6	610±10	5990±30	1.48
3		74.0±0.6		6170±30	1.48

attenuation coefficients (Barstow, 1985) and x-ray derived thicknesses for Lexan and aluminum (see table III).

This plot shows that the measured transmissions at wavelengths where the opacity is mainly due to the Lexan ($\lambda < 2000$ Å) are in good agreement with predictions. At longer wavelengths, where Lexan becomes transparent and the opacity is mainly due to aluminum, the measured transmissions are significantly higher than expected. The transmission value measured at 2537 Å (Hg Lamp) is 9×10^{-4}, about 100 times higher than expected. The transmission measured at 2300.6 Å (hollow cathode source, CO line) is 1.6×10^{-6}, also about 100 times higher than expected.

In order to verify that our results were not affected by stray light we repeated the measurement with a thick aluminum plate in place of the filter, and we measured no transmission. We also repeated the measurement at several filter positions, and got transmission values consistent with each other. An inspection of the above measured sample was then conducted with a microscope with 1 μm resolution to check the uniformity of the aluminum coating. This inspection showed that the

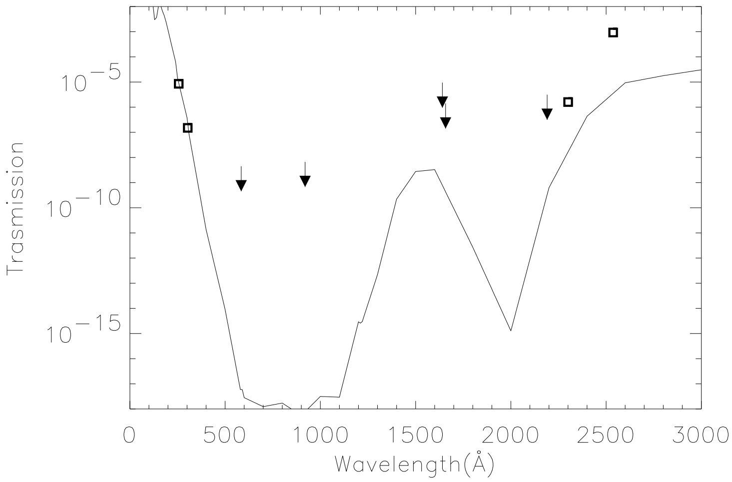

Figure 1. Vacuum UV transmission measurements of sample 1 (squares). Arrows indicate upper-limit to the transmission measurements. The superimposed curve is a simple slab transmission model adopting known linear attenuation coefficients (Barstow 1985) and x-ray derived thicknesses for Lexan and aluminum (see table 3).

aluminum coating was very uniform with no evidence of micro pin-holes that could be responsible for the observed higher UV transmission.

Puzzled by the unexpected results reported above, we made a series of additional and independent transmission measurements at the Physics Department of the University of Palermo. These measurements were performed in air using a Jasco model 5500 spectrophotometer covering the wavelength range 1900-8000 Å. The slits' aperture of the plane grating monochromator have been set in order to get a 10 Å FWHM pass band. Wavelength scans were taken with 20 Å steps and 400 Å/min speed. All samples in table I have been examined. Sample 2 has characteristics similar to sample 1, but with the aluminum coating only on one side. Sample 3 is a Lexan film with no coating.

Figure 2 shows the measured FUV/Visible transmission for sample 1 double-side aluminum coated (solid line), and sample 2 single-side aluminum coated (dashed line). Superimposed data points are the measurements taken at the XACT facility on sample 1 (crosses=measurements, arrows=upper limits).

We notice that the measurements taken at XACT on sample 1, at wavelengths longer than 2300 Å, are in very good agreement with measurements taken at the Physics Department (figures 2) and confirm the unexpected high transmission of the sample filter. The spectrophotometer is not able to measure transmission below $\sim 10^{-5}$, therefore, solid and dashed lines below 2300 Å are indeed upper limits. In addition, we notice that the transmission as a function of wavelength shows peaks and dips typical of interference effects (much more pronounced on sample 1). It

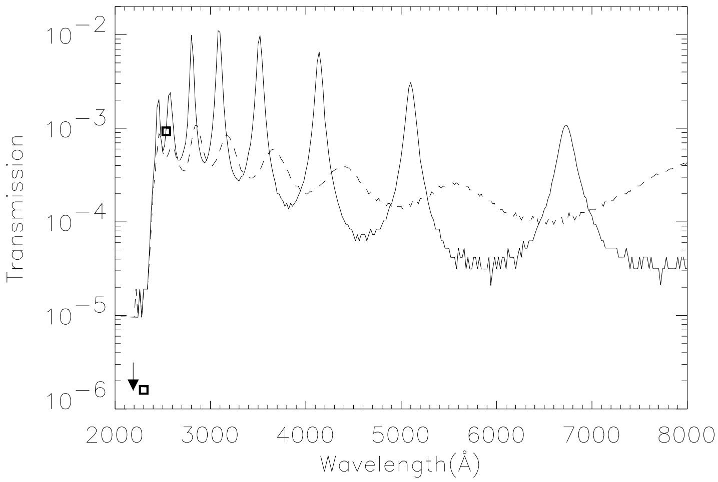

Figure 2. Measured transmission in the wavelength range 1900-8000 Å for double-side coating sample (sample 1, solid line), and single-side coating sample (sample 2, dashed line). Superimposed are the measurements taken on sample 1 at XACT facility (squares for measurements and arrow for the upper-limit).

is apparent that multilayer structures like those of our samples behave like Fabry-Perot interferometers. In such systems, at resonant wavelengths, transmission can be higher than the product of the transmission of each individual layer.

In the next section we briefly summarize a model of transmission for multilayer structures (Born and Wolf, 1984; Heavens, 1991) and compare predictions based on such a model with measured transmissions.

3. Modeling

The most general method of calculating the transmission T and reflection R of a multilayer for normal incidence radiation is based on a matrix formulation of the boundary conditions of the electromagnetic field. It can be shown (Born and Wolf, 1984; Heavens, 1991) that for the purposes of describing the propagation of a plane monochromatic wave through a stratified medium, the medium need only be specified by a 2×2 unimodular matrix (determinant = 1) M, usually referred to as the characteristic matrix of the stratified medium. If the stratified medium consists of N layers of thin films, the characteristic matrix of the whole medium is given by:

$$M = \prod_{j=1}^{N} M_j \tag{1}$$

with

$$M_j = \begin{bmatrix} cos(\delta_j) & i\ sin(\delta_j)/\eta_j \\ i\ \eta_j\ sin(\delta_j) & cos(\delta_j) \end{bmatrix} \tag{2}$$

and

$$\delta_j = \frac{2\,\pi}{\lambda}\, n_j\, d_j \tag{3}$$

where λ is the vacuum wavelength, $\eta_j = n_j - i\,k_j$ and d_j are the complex refractive index and thickness of the j-th layer, respectively.

If we define $\eta_{inc} = n_{inc} - i\,k_{inc}$, and $\eta_{exit} = n_{exit} - i\,k_{exit}$ the refractive indexes of the incident and exit media, respectively, the amplitude of the transmission and reflection coefficients t and r are given by:

$$t = \frac{2\,\eta_{inc}}{(X+W)\ +\ i\,(Y+V)} \tag{4}$$

$$r = \frac{(X-W)\ +\ i\,(Y-V)}{(X+W)\ +\ i\,(Y+V)} \tag{5}$$

where:

$$X = n_{inc}\ M_{11} - i\ n_{inc}\ k_{exit}\ M_{12} \qquad Y = -i\ n_{inc}\ n_{exit}\ M_{12}$$

$$W = n_{exit}\ M_{22} \qquad V = -i\ M_{21} - k_{exit}\ M_{22}$$

The intensity transmission and reflection coefficients T and R are:

$$T = \frac{n_{exit}}{n_{inc}}\ (|t|)^2 \tag{6}$$

$$R = (|r|)^2 \tag{7}$$

We can therefore calculate the transmission of any multilayer structure provided that the complex refractive index is known for each layer material.

4. Data Analysis and Discussion

Figure 3 and figure 4 show the transmission measurements taken in the 1900-6000 Å range (solid line) together with the predictions based on the above described model* (see equation [6]) adopting x-ray derived thicknesses of Lexan and aluminum (see table III) (dashed-dotted line), and best fit Lexan and aluminum thicknesses (dashed line).

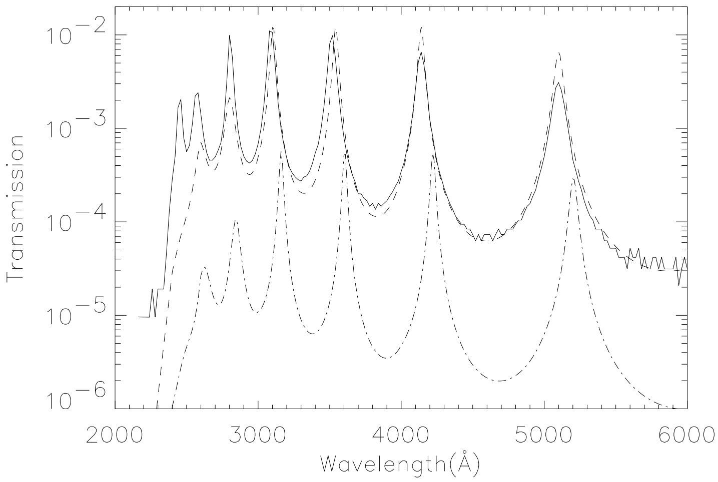

Figure 3. Measured transmission in the wavelength range 1900-6000 Å for the double-side coating sample (sample 1, solid line). Superimposed is the model transmission with nominal thickness of Lexan and aluminum (dashed-dotted line), and the best-fit model transmission (dashed line).

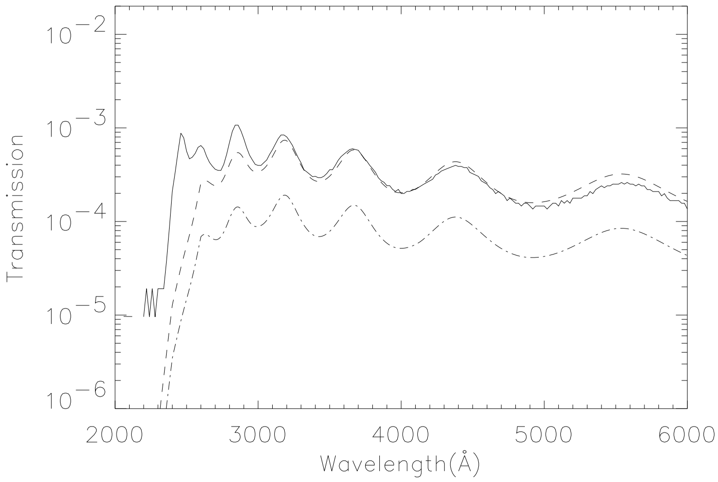

Figure 4. Measured transmission in the wavelength range 1900-6000 Å for the single-side coating sample (sample 2, solid line). Superimposed is the model transmission with nominal thickness of Lexan and aluminum (dashed-dotted line), and the best-fit model transmission (dashed line).

The best-fit model parameters obtained by interactive adjustments are summarized in table IV lines 1 and 2. Lexan thicknesses derived above are in reason-

* The complex refractive indexes used in the model are taken from (Hageman et al., 1974) for aluminum and from (Barstow, 1985; Altman, 1995) for Lexan.

Table IV
Thickness (Å) of Lexan and aluminum derived from a best-fit analysis of the FUV/Visible transmission measurements adopting a multilayer transmission model.

Sample 1		Sample 2		Sample 3	
Al	*Lexan*	*Al*	*Lexan*	*Al*	*Lexan*
510	6130	525	5990		6130

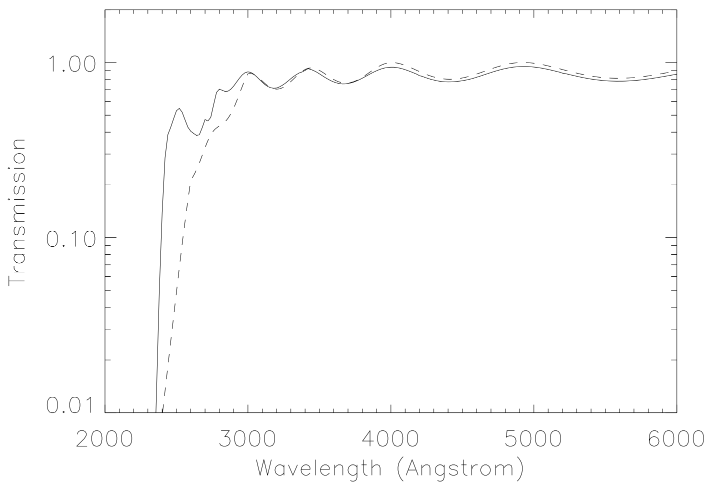

Figure 5. Measured transmission in the wavelength range 1900-6000 Å for a Lexan sample (sample 3, solid line). Superimposed is the best-fit model transmission (dashed line).

able agreement with those derived from x-ray measurements (see table III), while derived thicknesses of aluminum are significantly lower.

Figure 5 shows the FUV/Visible transmission measurements conducted on a sample of pure Lexan with the spectrophotometer (solid line).

Interference effects due to reflections at the interface between the plastic film and air are still present, but much less significant. The superimposed dashed line curve is the model for a single layer of Lexan with Lexan thickness derived from x-ray measurements (table III). This thickness is equal to that derived optimizing the interferences model to fit the FUV/Visible transmission measurements (table IV, line 3), thus proving the validity of our approach and suggesting that aluminum is responsible for the observed discrepancy between x-ray and FUV/Visible thickness measurements in samples 1 and 2. Notice that at wavelengths shorter than 2600 Å the refractive index of Lexan is only poorly known, and this probably is the reason for the measured transmission being higher than predicted.

One possible interpretation of the significant discrepancy between thicknesses of aluminum derived from x-ray measurements and those derived from FUV/Visible

Table V
Best Fit results on synchrotron x-ray transmission measurements obtained adopting an x-ray transmission model which includes aluminum, Lexan, and Al_2O_3

Sample	Mass Areal Density ($\mu g\ cm^{-2}$)			Thickness (Å)			χ^2
	Al	Lexan	Al_2O_3	Al	Lexan	Al_2O_3	
1	15.7 ± 0.3	74.0 ± 0.3	4.4 ± 0.4	630 ± 10	6160 ± 100	110 ± 10	1.04
2	14.2 ± 0.3	71.3 ± 0.3	1.7 ± 0.4	570 ± 10	5940 ± 30	40 ± 10	1.18

measurements is that oxidation of the exposed surface of aluminum alters its properties making the oxide layer more transparent in the UV/visible wavelength range, and thus reducing the effective (in terms of UV rejection) layer of aluminum. We also cannot exclude the possibility that chemical reactions occur at the plastic-aluminum interface that also affect the optical properties of aluminum.

In the extreme hypothesis that only oxidation is responsible for the observed higher FUV/Visible transmission, and aluminum oxide is completely transparent to FUV/Visible radiation (Smith et al., 1985), aluminum thicknesses derived from FUV/Visible measurements (table IV), compared to those derived from x-ray measurements (table III), are consistent with a layer of oxide of 110 Å on each exposed surface of aluminum for sample 1, and an oxide layer of 85 Å on the exposed surface of aluminum on sample 2.

The oxidation of aluminum does not change the x-ray transmission of aluminum, but the addition of oxygen, in principle, does. We have tried to fit the x-ray transmission measurements taken at BESSY synchrotron on sample 1 and 2 (Barbera et al., 1996) including aluminum oxide in the transmission model. The results of this least χ^2 fitting procedure are reported in Table V giving mass areal densities of Lexan, aluminum and aluminum oxide, thicknesses derived adopting densities of 1.2, 2.5, and 3.97 $g\ cm^{-3}$ for Lexan, aluminum, and aluminum oxide, respectively. The last column of table V is the χ^2 value (372 degrees of freedom).

These fitting results show that:

1. The χ^2 of the fitting (table V) is significantly lower when aluminum oxide is included in the transmission model (for comparison see table III).
2. The thickness of aluminum oxide in sample 1 (double side coating) is more than twice the value obtained in sample 2 (single side coating) thus confirming results of the FUV/Visible transmission measurements.
3. The thickness of Lexan in sample 1 derived from x-ray measurements adopting a model that includes aluminum oxide (table V) is much closer to the value derived from FUV/Visible measurements (table IV). For comparison see derived Lexan thickness of sample 1 reported in table III.

The fact that absolute values of aluminum oxide thicknesses derived from x-ray and FUV/Visible measurements do not match each other may be due to the actual density of aluminum oxide being lower than the adopted value of 3.97 $g\ cm^{-3}$.

Table VI

Summary of thickness values (Å) of Lexan and aluminum for the three samples considered in this paper. Line 1 gives manufacturer values, line 2 values derived from UV/Visible transmission measurements. Values derived from synchrotron X-ray transmission measurements are reported in line 3 (adopting a transmission model which includes only Lexan and aluminum), and in line 4 (adopting a transmission model which also includes the presence of Al_2O_3).

Source	Sample 1			Sample 2			Sample 3
	Lexan	Al	Al_2O_3	Lexan	Al	Al_2O_3	Lexan
Luxel Corp.	6065±100	705±70		5805±100	710±50		5740±100
UV/Visible	6130	510	225	5990	525	85	6130
X-ray	6290±100	730± 10		5990±30	610± 10		6170±30
X-ray (Al_2O_3)	6160±100	630±10	110±10	5940±30	570±10	40±10	

We cannot, however, exclude the possibility that some interaction at the interface between plastic and aluminum occurs that also affects the UV/Visible opacity of aluminum.

Table (VI) summarizes the different thickness values reported in this paper for the three samples.

5. Results and Conclusions

The reported UV transmission measurements conducted on the two samples of aluminum coated Lexan show that the UV rejection at wavelengths longer than about 2300 Å is significantly lower (more than two orders of magnitude) than the expected performance. On the basis of EUV measurements conducted on sample 1 at 256, 304, and 584 Å, where aluminum is basically transparent, and on the basis of FUV/Visible measurements conducted on sample 3, the performance of pure Lexan turns out to be nominal.

Transmission significantly higher than expected occurs at wavelengths ($\lambda >$ 2300 Å) where Lexan is nearly transparent and opacity is due to aluminum. Inspections conducted with a microscope with 1 μm resolution have shown that the aluminum coating is very uniform with no evidence of micro pin-holes that could be responsible for the observed higher UV transmission.

Constructive interferences in transmission occur at resonant wavelengths due to the multilayer design of coated membranes. Interference effects in transmission occur in all samples analyzed, being more prominent in the sample with an aluminum coating on both sides (figure 2 solid line), but still present in the single-side coated sample (figure 2 dashed line), and, to a lesser degree, in plastic membranes with no aluminum coating (figure 5).

Modeling the observed FUV/Visible transmission of coated Lexan samples, taking into account interferences due to the multilayer design of the filters, we have found that, in addition to a decrease of average opacity due to interference effects, aluminum UV/Visible opacity is significantly lower than expected.

As a possible interpretation we suggest that oxidation of exposed aluminum surfaces significantly affects UV opacity, while x-ray transmission is affected only by the presence of the small amount of oxygen in the aluminum oxide. Using x-ray transmission measurements conducted at BESSY synchrotron on all analyzed samples (Barbera et al., 1996), we find that taking into account aluminum oxide significantly improves the x-ray transmission modeling.

According to our modeling and measured transmission we estimate that an effective layer of nearly 2 $\mu g/cm^2$ of aluminum oxide (Al_2O_3) forms on each exposed surface of aluminum. This effect is thus more significant for filters with aluminum coatings on both sides.

The results of this work conducted in the framework of the calibration of the AXAF-HRC UV/Ion shields have led to a redesign of the shields itself. These results have also suggested a possible explanation of the leaks at UV wavelengths observed in the ROSAT HRI (Zombeck et al., 1995). In another paper (Zombeck et al., 1996) we discuss this issue in detail.

Acknowledgements

We thank Prof. Claudio Arnone and dr. Giuseppe Lullo for their useful comments and suggestions to this work. We acknowledge support by Agenzia Spaziale Italiana and Ministero della Università e della Ricerca Scientifica e Tecnologica (MB, AC, AD, ML, SS, SV), NASA contract NAS8-38248 (MVZ). We thank INTEC s.r.l., Palermo, for their technical support in setting up a clean environment for sample handling and measurements.

References

Altman, R.M., 1995, in "Designing Plastic Optics: New Applications Emerging for Optical Glass Substitutes", C. Tribastone, C. Teyssier, and W. Peck, OPKOR, Inc., The Photonics Design & Applications Handbook, Laurin Publishing Co., Inc. , Pittsfield, MA.

Barbera, M., Collura, A., Dara, A., 1995, OAPA internal report, document number OAPA-R3-1995.

Barbera, M., Collura, A., Dara, A., 1996, *SPIE Proc.*, **Vol. 2808** in press.

Barstow, 1985, University of Leicester internal report.

Born and Wolf, 1984, "Principles of Optics", Pergamon Press.

Bowyer, S., et al., 1992, *Bull. American Astron. Soc.*, **181, 23.02**

Collura, A., Barbera, M., Inzerillo, G., Mirabello, F., Sciortino, S., Serio, S., 1994, *SPIE Proc.*, **Vol. 2280**, p. 206.

Collura, A., Barbera, A. Dara, M., Inzerillo, G., Mirabello, F., Sciortino, S., Serio, S., 1996, *SPIE Proc.*, **Vol. 2808**, in press.

Fabricant, D.G., et al., 1979, *Rev. Sci. Inst.*, **50**, 727.

Heavens, O.S., 1991, "Optical Properties of Thin Films", Dover Publications, New York

Hagemann, Gudet, and Kunz, 1974, DESY report SR-74/7.

Malina, R. F., et al., 1992, *Bull. American Astron. Soc.*, **181, 23.01**

Murray, S.S., and Chappel, J.H., 1985, *SPIE Proc.*, **Vol. 597**, p. 274.
Smith, D.Y., Shiles, E., and Mitio Inokuti, in "Handbook of optical constants of solids", p. 369-406, Ed. Palik, E.D., Academic. Press, Inc.
Taylor, B., Andresen, R., Peacock, A., Zobl, R., 1981, *Space Sci. Rev.*, **Vol. 30**, p. 479.
Truemper, J., 1983, *Adv. Space Res. 2*, **N. 4**, p. 241.
Vallerga, J., Siegmund, O.H.W., Everman, E., and Jelinsky, P., 1986, *Proc. SPIE*, **Vol. 689**, p. 138.
Weisskopf, M., 1985, *Proc. SPIE*, **Vol. 597**, p. 228.
Weisskopf, M., 1996, *Proc. SPIE*, **Vol. 2808**, in press.
Zombeck, M.V., David. L.P., Harnden, F.R., Jr., and Kearns, K., 1995, *SPIE Proc.*, **Vol. 2518**, p. 304.
Zombeck, M.V., et al., 1996, in preparation.

Address for correspondence: Osservatorio Astronomico G.S. Vaiana, Palazzo dei Normanni, 90134 Palermo, Italy